Dual coding potential of a 2′,5′-branched ribonucleotide in DNA

JESSICA DÖRING and THOMAS HUREK

Department of Microbe-Plant Interactions, CBIB (Center for Biomolecular Interactions Bremen), University of Bremen, D-28334 Bremen, Germany

ABSTRACT

Branchpoints in RNA templates are highly mutagenic, but it is not known yet whether this also applies to branchpoints in DNA templates. Here, we report how nucleic acid polymerases replicate a 2′,5′-branched DNA (bDNA) molecule. We constructed long-chained bDNA templates containing a branch guanosine and T7 promoters at both arms by splinted ligation. Quantitative real-time PCR analysis was used to investigate whether a branchpoint blocks DNA synthesis from the two arms in the same manner. We find that the blocking effect of a branchpoint is arm-specific. DNA synthesis from the 2′-arm is more than 20,000-fold decreased, whereas from the 3′-arm only 15-fold. Our sequence analysis of full-length nucleic acid generated by Taq DNA polymerase, Moloney murine leukemia virus reverse transcriptase, and T7 RNA polymerase from the 2′-arm of bDNA shows that the branched guanine has a dual coding potential and can base-pair with cytosine and guanine. We find that branchpoint templating is influenced by the type of the surrounding nucleic acid and is probably modulated by polymerase and RNase H active sites. We show that the branchpoint bypass by the polymerases from the 3′-arm of bDNA is predominantly error-free, indicating that bDNA is not as highly mutagenic as 2′,5′-branched RNA.

Keywords: 2′,5′-branched DNA; arm-specific branchpoint blocking; dual coding potential; error-free branchpoint bypass; templating branchpoint

INTRODUCTION

DNA and RNA polymerases are template-dependent enzymes that catalyze nucleotide polymerization according to Watson–Crick base-pairing rules. DNA polymerases are classified into several different families (A, B, C, D, X, Y, and reverse transcriptase [RT]) based on primary amino acid sequence similarities (Trakselis and Murakami 2014). RNA polymerases decrease into two distinct classes: (i) the single-subunit and (ii) the multisubunit proteins (Cheetham and Steitz 2000; Cramer 2002). RTs of retroviruses and long terminal repeats (LTR) retrotransposons constitute a special class of DNA polymerases. These RTs possess an N-terminal polymerase domain and a C-terminal RNase H domain (Le Grice and Nowotny 2014). Despite differences in primary sequence, template and nucleotide selectivity, DNA and single-subunit RNA polymerases share a common general structure of their polymerase domains (Sousa 1996). The polymerase domains are composed of three subdomains referred to fingers, thumb, and palm (Ollis et al. 1985). The palm subdomain is the catalytic domain containing three highly conserved aspartate residues that bind two magnesium ions required for catalysis, the fingers and thumb subdomains have principal roles in nascent base-pair and template–primer binding, respectively (Joyce and Steitz 1995).

DNA polymerases must be highly accurate when copying genomic DNA templates during replication in order to maintain genetic information (Kornberg and Baker 1992). However, physical and chemical insults, including radiation, xenobiotics, chemical carcinogens, and reactive oxygen species (ROS) compromise the coding potential of DNA by producing modified nucleosides (DNA lesions) that interfere with replication and transcription (Brieba et al. 2005). For example, the well-studied DNA lesion 8-Oxo-7,8-dihydro-2′-deoxyguanosine (8-oxo-dG) generated by ROS-mediated oxidation of guanine (Beckman and Ames 1997) has a dual coding potential because it templates the insertion of dCMP and dAMP during DNA synthesis by DNA polymerases (Brieba et al. 2004). Notably, structural studies revealed that DNA polymerases modulate the coding potential of this noncanonical

Corresponding author: thurek@uni-bremen.de

Article is online at http://www.rnajournal.org/cgi/doi/10.1261/rna.068486.118.

nucleotide by determining which of the two bases will be inserted opposite to it (Krahn et al. 2003; Brieba et al. 2004, 2005; Rechkoblit et al. 2006; Zang et al. 2006; Eoff et al. 2007; Batra et al. 2012; Freudenthal et al. 2013a).

Another well-known noncanonical nucleotide is a branched ribonucleotide (branched nucleotide, branchpoint) from which two nucleic acid strands branch out into a 2′-arm and a 3′-arm via vicinal 2′,5′ and 3′,5′ phosphodiester bonds, respectively (Wallace and Edmonds 1983; Nam et al. 1994). They are found in spliceosomal and group II intron RNA lariats (Kruger et al. 1982; Padgett et al. 1984), in 2′,5′-branched RNA/DNA chimeric molecules (multicopy single-stranded DNAs) (Hsu et al. 1989), in mRNA (Nielsen et al. 2005), and presumably in the genomic RNA of retroviruses and LTR retrotransposons (Cheng and Menees 2004; Galvis et al. 2017). However, the branchpoint in genomic RNAs is controversially discussed (Coombes and Boeke 2005, Pratico and Silverman 2007) because direct evidence for this nucleotide is lacking. It was found that branched nucleotides in RNA are highly mutagenic because the branchpoint triggers single mismatch errors and/or deletion mutations in RT-synthesized complementary DNAs (cDNAs) (Vogel et al. 1997; Tuschl et al. 1998; Vogel and Börner 2002; Gao et al. 2008; Bitton et al. 2014; Mercer et al. 2015; Döring and Hurek 2017). Based on these studies, we asked whether a branched ribonucleotide embedded in DNA has the same mutagenic character. To address this question, we constructed a long- and open-chained 2′,5′-branched DNA (bDNA) oligonucleotide by splinted ligation (Fig. 1; Mendel-Hartvig et al. 2004). This bDNA molecule allowed us to examine how a family A DNA polymerase (Taq DNA polymerase, Taq) and a member of the RT family (Moloney murine leukemia virus [M-MLV] RT with [H+] and without [H−] RNase H activity) replicate at a branched nucleotide during DNA synthesis from the 2′- and 3′-arm. To investigate how a single-subunit RNA polymerase (T7 RNA polymerase, T7 RNAP) transcribes bDNA, we equipped both arms of our bDNA with a T7 promoter. To compare the mutation profile of our bDNA to that of our previous 2′,5′-branched RNA (bRNA) (misinsertion of dGMP opposite to the branch guanosine) (Döring and Hurek 2017), we synthesized the bDNA molecule to contain the same sequence and branched nucleotide as the bRNA molecule (Döring and Hurek 2017). This also allowed us to compare replication at the branch guanosine in both molecules by RT, which can use RNA and DNA as templates for synthesis (Le Grice and Nowotny 2014). It is well established that branched nucleotides in RNA templates are obstacles to RT-catalyzed DNA synthesis (Krainer et al. 1984; Rodriguez et al. 1984). We asked whether a branchpoint blocks DNA synthesis from the two arms in the same manner. To address this question, we carried out quantitative real-time PCR (qPCR) analysis on our bDNA construct.

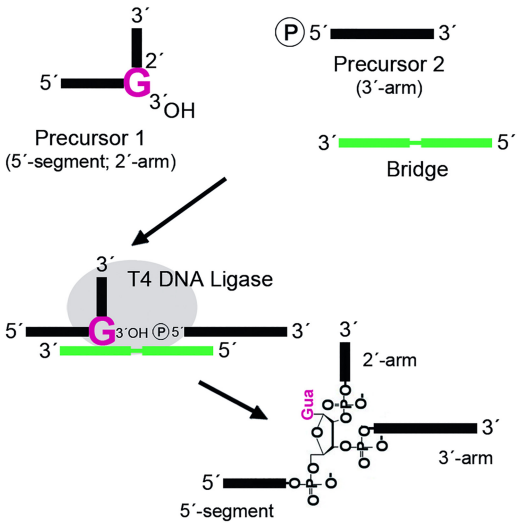

FIGURE 1. Scheme of the splinted ligation method to construct branched DNA. Briefly, a unique 2′,5′-linked ribo-guanosine (G)-nucleoside in a DNA strand representing the 5′-segment and 2′-arm (precursor 1) is transformed into a branched nucleotide by ligation to a DNA strand representing the 3′-arm (precursor 2). To achieve this, the two precursors are partially annealed to a complementary DNA bridge. Thus, the free 3′ hydroxyl of the 2′,5′-linked nucleoside of precursor 1 is brought close to the 5′ phosphate of precursor 2. The two oligonucleotides are then ligated by T4 DNA Ligase. The bDNA construct with the branch guanosine is shown on the *right*. Black and green lines represent DNA. The 2′,5′-linked ribo-G-nucleoside in precursor 1 and in bDNA is shown in magenta and is highlighted. Nucleic acids downstream from a 2′,5′ phosphodiester bond are plotted *vertically* in linear and branched oligonucleotides.

We found that the branched ribonucleotide in the bDNA molecule exhibits a dual coding potential and is not highly mutagenic. Our sequence analysis of 2′-arm-specific full-length nucleic acid generated by Taq, M-MLV RTs, and T7 RNAP showed that the branch guanosine templates for the insertion of the correct partner, dCMP/CMP [(d)CMP], and incorrect partner, dGMP/GMP [(d)GMP]. Moreover, we observed that the coding potential of the branchpoint is modulated by polymerase active sites and, surprisingly, in M-MLV RT also by RT's RNase H. Furthermore, our sequence analysis of arm-specific full-length DNAs from bRNA and bDNA revealed that the coding potential of a branchpoint depends on whether the surrounding nucleotides are RNA or DNA. Using qPCR analysis, we quantified the branchpoint blocking effect on DNA synthesis and found that blocking is more pronounced when DNA polymerase bypasses the branch guanosine from the 2′-arm than from the 3′-arm of our bDNA. Our sequence analysis of 3′-arm-specific full-length complementary nucleic acids showed a predominantly error-free branchpoint bypass by the polymerases. This indicates that branched ribonucleotides in DNA are not as highly mutagenic as their counterparts in RNA.

RESULTS

Using branched DNAs for primer extension and in vitro transcription analysis

In total, we prepared three types of bDNAs: (i) native bDNA, (ii) bDNA with a T7 promoter at its 2′-arm, and (iii) bDNA with a T7 promoter at its 3′-arm (Fig. 2). To compare how wild-type and RNase H-deficient M-MLV RT, Taq, and T7 RNAP read a branchpoint, we constructed the three bDNAs to contain the same sequence and branched nucleotide.

The branched nucleotide is an obstacle to DNA synthesis (Krainer et al. 1984; Rodriguez et al. 1984) and because of this, RTs generate two cDNAs from bRNA: (i) truncated cDNA until the branchpoint and (ii) full-length cDNA through the branchpoint (Tuschl et al. 1998; Conklin et al. 2005; Döring and Hurek 2017). To demonstrate that Taq and M-MLV RTs produce these two DNAs as well, we performed primer extension analysis from both arms of our native bDNA using the 2–5 and 3–5 reverse primers (Fig. 2A). To show that T7 RNAP transcribes the bDNA template until the branched nucleotide and through the branched nucleotide, we carried out in vitro transcription analysis using our bDNA containing a T7 promoter at the 2′-arm (Fig. 2B) or at the 3′-arm (Fig. 2C). To confirm that the nucleic acid enzymes synthesized DNA/RNA through the branch guanosine, we carried out hybridization analysis using a specific probe (probe fl). Probe fl is complementary to synthesized RNA or DNA downstream from the 2′,5′-linked ribo-G-nucleoside in precursor 1 and in bDNA (Supplemental Fig. S1). This probe detects both full-length RNA/DNA synthesized from the 2′- and 3′-arm of bDNA, as well as

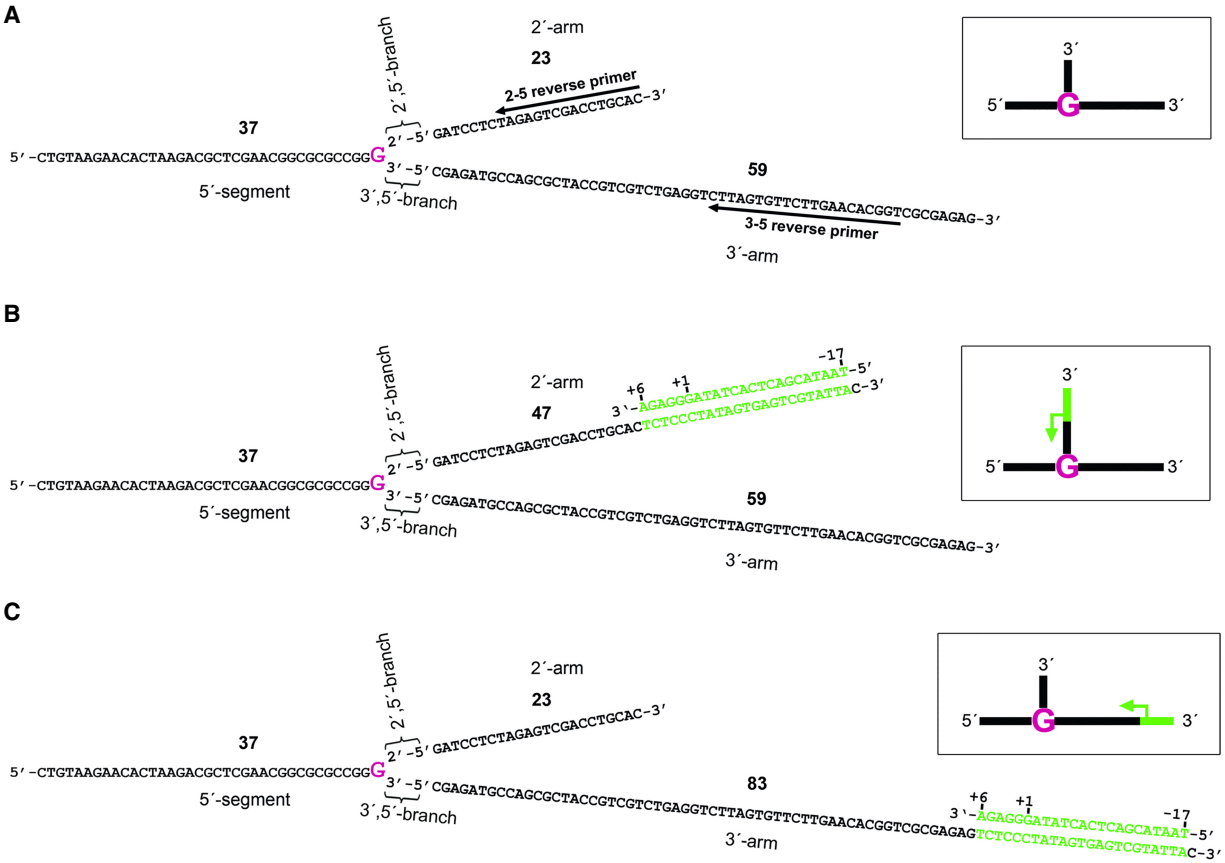

FIGURE 2. Branched DNA oligonucleotides. (*A*) Sequence and length of the native bDNA construct. This bDNA consists of a 37-mer 5′-segment, a 23-mer 2′-arm, and a 59-mer 3′-arm. The branchpoint nucleotide guanosine (branch guanosine) is highlighted in magenta. Black nucleotides represent DNA. Numbers refer to the length in nucleotides of the respective nucleic acid. Reverse primer binding sites are indicated by arrows. The 2–5 and 3–5 reverse primers were used to prime DNA synthesis from the 2′- and 3′-arm, respectively. (*B*) Sequence and length of the bDNA construct with a T7 promoter at its 2′-arm. This bDNA is composed of a 37-mer 5′-segment, a 47-mer 2′-arm, and a 59-mer 3′-arm. Colors and numbers as in panel *A*. Green nucleotides represent the double-stranded T7 promoter region. Numbers *above* the region refer to the nucleotide positions in the T7 promoter sequence, where +1 indicates the start of transcription. (*C*) Sequence and length of the bDNA construct with a T7 promoter at its 3′-arm. This bDNA consists of a 37-mer 5′-segment, a 23-mer 2′-arm, and a 83-mer 3′-arm. Colors and numbers as in panel *A*; green nucleotides and numbers *above* them as in panel *B*. The orientation of the shown bDNA constructs is defined as "sense." The 2′,5′- and 3′,5′-phosphodiester bonds of branch guanosines are defined as 2′,5′- and 3′,5′-branches, respectively. A schematic presentation of the respective bDNA oligonucleotide that will be used in the following figures is boxed in black. The green arrow shows the start site and orientation of transcription.

full-length DNA from precursor 1. Hybridizing full-length DNAs/RNAs were purified from the gel and amplified by PCR for subsequent sequence analysis to investigate how the enzymes read the branch guanosine.

M-MLV RTs and Taq polymerize through the branchpoint from the 2′-arm of bDNA

Our primer extension analysis from the 2′-arm of bDNA using the 2–5 reverse primer showed that all DNA polymerases produced truncated DNAs of 23 nucleotides (nt) in length until the 2′,5′-branch (Supplemental Fig. S2, left panel). Unfortunately, full-length DNAs with a length of 60 nt were not clearly visible in the denaturing gel (Supplemental Fig. S2, left panel), indicating that the enzymes are unable to efficiently bypass the branchpoint. To detect full-length DNAs, we carried out hybridization analysis. Hybridization analysis showed that all DNA polymerases were able to read through the branched nucleotide (Supplemental Fig. S2, right panel). To improve the visibility of full-length DNAs on the gel, we separated the primer extension products in a nondenaturing gel since dsDNA (duplex between DNA and template) is more susceptible to intercalating dyes than single-stranded (ss) DNA. Two product bands per primer extension reaction were visible on the gel. The lower product band was determined as a duplex between truncated DNA until the 2′,5′-branch and bDNA using constructed duplexes as size markers (Fig. 3A, left panel). The upper product band was identified as a duplex between full-length DNA through the 2′,5′-branch and bDNA (full-length duplex) by hybridization analysis (Fig. 3A, right panel). Full-length duplexes were excised from the gel and subjected to PCR. The presence of bDNA during the PCR reaction cannot interfere with our sequence analysis of full-length amplicons because the branch guanosine strongly inhibits amplification of bDNA from the 2′-arm (see below). Linear DNA, therefore, will be favored over bDNA as template in the PCR reaction.

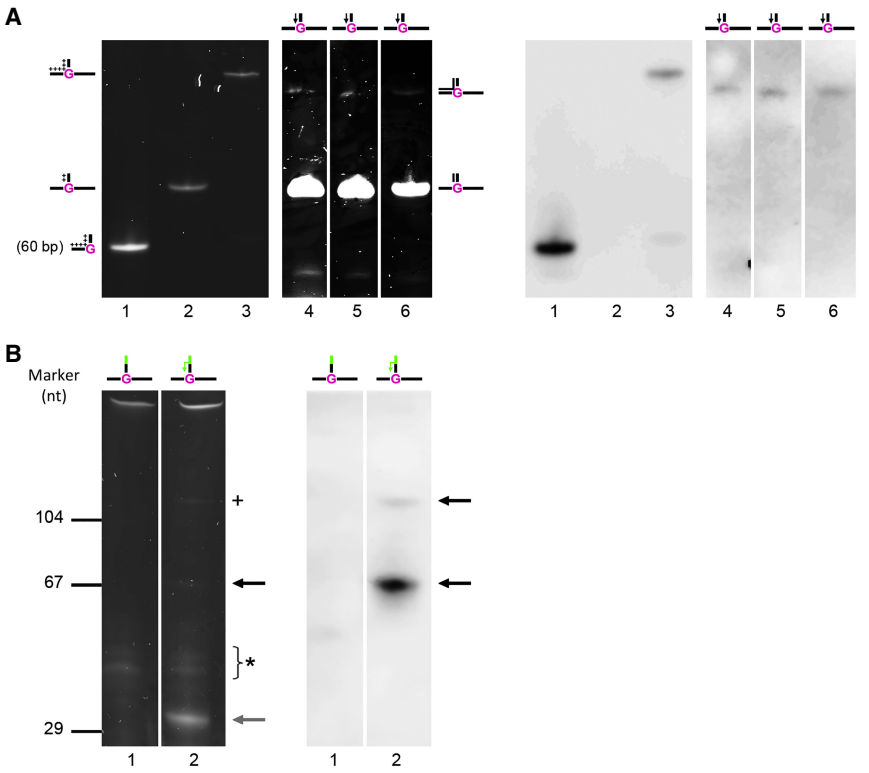

FIGURE 3. Detection of full-length DNA and RNA through the 2′,5′-branch by probe hybridization. (*A*) Primer extension analysis from the 2′-arm of bDNA. Samples were separated on a nondenaturing 12% polyacrylamide gel; bp, base pairs. (Lane *1*) Duplex between precursor 1 and oligonucleotide representing full-length DNA. (Lane *2*) Duplex between bDNA and oligonucleotide representing truncated DNA until the 2′,5′-branch. (Lane *3*) Duplex between bDNA and oligonucleotide representing full-length DNA. (Lane *4*) Primer extension reaction from the 2′-arm of bDNA using Taq. (Lanes *5*, *6*) Primer extension reactions from the 2′-arm of bDNA using M-MLV RT (H+) and (H−), respectively. The black arrow in the pictogram depicts the primer-target region and direction of primer extension. Duplexes from lanes *1–3* are schematically illustrated on the *left* of the gel, where pluses in pictograms indicate the oligonucleotide representing truncated or full-length DNA. Double-stranded primer extension products are schematically illustrated on the *right* of the gel, where the solid line in pictograms represents the synthesized DNA. Nucleic acids shown on the *left* were blotted and hybridized with probe fl (*right* panel). This probe is specific for full-length RNA and DNA of bDNA, as well as full-length DNA from precursor 1. (*B*) In vitro transcription analysis from the 2′-arm of bDNA. (Lane *1*) Negative control for in vitro transcription reaction. (Lane *2*) In vitro transcription reaction from the 2′-arm of bDNA using T7 RNA polymerase. Green arrow in pictogram as in Figure 2. The full-length run-off transcript is labeled with a black arrow and truncated RNA until the 2′,5′-branch with a gray arrow. The transcription side-product is indicated by a plus. By-products in solid-phase synthesis of the T7 primer are labeled with an asterisk. Heat-denatured samples were separated on a 15% denaturing polyacrylamide gel (*left*), blotted and hybridized with probe fl (*right*). Probe specificity as in panel *A*. Hybridizing RNAs are labeled with an arrow. Due to their unusual shape, bDNA oligonucleotides exhibit an anomalous electrophoretic mobility in denaturing urea polyacrylamide gels and migrate more slowly than their corresponding linear oligonucleotides (oligonucleotides containing the 5′-segment and 3′-arm) (Ruskin et al. 1984; Ruskin and Green 1985). Colors as in Figure 1.

Interestingly, full-length duplexes generated by the DNA polymerases migrated faster in the gel than the constructed one (Fig. 3A, lanes 3–6). We assumed that the oligonucleotide representing full-length DNA through the 2′,5′-branch cannot properly hybridize to the branched region of bDNA. This presumably leads to a loop formation

at the branched region, which may slow down migration of the constructed full-length duplex in the gel.

T7 RNAP reads through the branchpoint from the 2′-arm of bDNA

In vitro transcription analysis using bDNA containing a T7 promoter at the 2′-arm revealed that T7 RNAP generated two RNA molecules from our bDNA: a truncated transcript of 29 nt in length and a full-length "run-off" transcript of 66 nt in length (Fig. 3B, left panel). Hybridization analysis confirmed that T7 RNAP synthesizes RNA through the branchpoint (Fig. 3B, right panel).

An RNA molecule of a larger size than the run-off transcript was produced during the in vitro transcription reaction (Fig. 3B, left panel, lane 2). Hybridization with probe fl (Fig. 3B, right panel, lane 2) revealed that this transcription side-product contained full-length RNA. This was also confirmed by RT-PCR using the forward and 2–5 reverse primers (Supplemental Fig. S3A, lane 5). Because of its large size (>104 nt), the side-product was presumably generated by the RNA-dependent polymerization activity of T7 RNAP (Supplemental Fig. S4; Cazenave and Uhlenbeck 1994; Lehmann et al. 2007).

M-MLV RTs and Taq read through the branchpoint from the 3′-arm of bDNA

Primer extension analysis from the 3′-arm of bDNA using the 3–5 reverse primer showed that M-MLV RTs produced full-length (88 nt) and truncated (51 nt) DNA from our bDNA (Fig. 4A, left panel). We confirmed synthesized DNA through the branch guanosine by hybridization analysis (Fig. 4A, right panel). To show that Taq can read through the branchpoint during DNA synthesis from the 3′-arm, we carried out a PCR reaction using the forward and 3–5 reverse primers (Supplemental Fig. S5B, lane 2).

T7 RNAP polymerizes through the branchpoint from the 3′-arm of bDNA

In vitro transcription with bDNA containing a T7 promoter at the 3′-arm revealed that T7 RNAP generated a truncated transcript of 65 nt in length and a full-length "run-off" transcript of 102 nt in length (Fig. 4B, left panel). Hybridization analysis confirmed the T7 RNAP-synthesized RNA through the branch guanosine (Fig. 4B, right panel). Hybridization and PCR analysis (Fig. 4B, right panel, lane 2; Supplemental Fig. S3B, lane 5) revealed that, similar to in vitro transcription from the 2′-arm, a side-product was generated by T7 RNAP (Cazenave and Uhlenbeck 1994).

Nucleic acid polymerases read the branchpoint in bDNA in an error-free and error-prone manner

Recently, we have constructed a bRNA molecule containing the same sequence and branched nucleotide as the bDNA molecule used here. Our previous work on this bRNA molecule had shown that M-MLV RT (H−) reads differently the branch guanosine through the 2′,5′- than

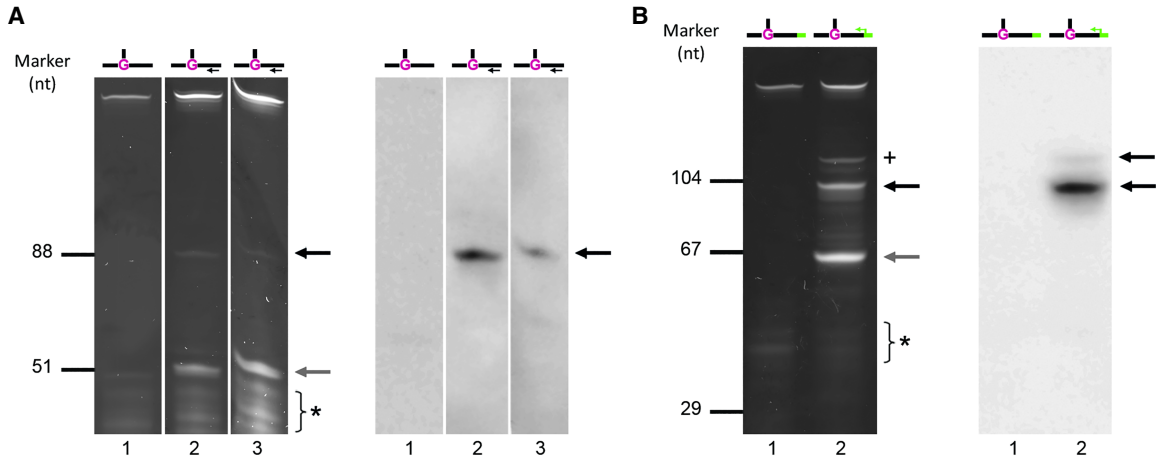

FIGURE 4. Detection of full-length DNA and RNA through the 3′,5′-branch by probe hybridization. (*A*) Primer extension analysis from the 3′-arm of bDNA. (Lane *1*) Negative control for primer extension reaction. (Lanes *2, 3*) Primer extension reactions from the 3′-arm of bDNA using M-MLV RT (H+) and (H−), respectively. Arrows in pictograms as in Figure 3A. Full-length DNA through the 3′,5′-branch is labeled with a black arrow and truncated DNA until the 3′,5′-branch with a gray arrow. Asterisk indicates by-products in solid-phase synthesis of the 3–5 reverse primer. Samples were heat-denatured and electrophoresed on a 15% denaturing polyacrylamide gel (*left* panel), blotted and hybridized with probe fl (*right* panel). Probe specificity as in Figure 3A. Hybridizing full-length DNA is indicated by an arrow. (*B*) In vitro transcription analysis from the 3′-arm of bDNA. (Lane *1*) Negative control for in vitro transcription reaction. (Lane *2*) In vitro transcription reaction from the 3′-arm of bDNA using T7 RNA polymerase. Green arrow in pictogram as in Figure 2; plus, black and gray arrow as in Figure 3C. Asterisk indicates by-products in solid-phase synthesis of T7 primer. Samples were heat-denatured and separated on a 15% denaturing polyacrylamide gel (*left*), blotted and hybridized with probe fl (*right*). Probe specificity as in Figure 3A. Hybridizing full-length RNAs are labeled with an arrow. Colors as in Figure 1.

through the 3′,5′-branch (Döring and Hurek 2017). When M-MLV RT (H–) bypasses the branch guanosine from the 2′-arm, the enzyme incorporates predominantly dGMP opposite to the branchpoint. Because of this misincorporation, sequenced PCR products contain a cytidine at the position of the branch guanosine (G→C transversion) in the sense-strand. In the course of a bypass from the 3′-arm, the enzyme misincorporates dGMP and additionally skips one to several template nucleotides located upstream of the branchpoint. Because of this misreading, sequenced PCR amplicons contain a G→C transversion and deletions in the sense-strand (Döring and Hurek 2017).

Here, we wanted to investigate how wild-type and RNase H-deficient M-MLV RT, Taq and T7 RNAP read the branch guanosine in bDNA from both arms. Furthermore, we wanted to know if these polymerases differ from each other in their processing of the branch guanosine. For this purpose, we sequenced amplified full-length DNAs (Supplemental Fig. S5) and RNAs (Supplemental Fig. S3) through the 2′,5′- and 3′,5′-branch. Full-length DNA/RNA through the 2′,5′- and 3′,5′-branch are designated as 2′-arm- and 3′-arm-specific DNA/RNA, respectively. The sequencing reads surrounding the branch guanosine obtained from cloned amplicons of 2′- and 3′-arm-specific DNAs and RNAs are shown in Supplemental Tables S1–S8. The most common mutations of the branchpoint found in arm-specific DNAs generated by these polymerases after cloning are presented in Table 1. Table 1 illustrates that, similar to bRNA (Döring and Hurek 2017), the nucleic acid polymerases misincorporated (d)GMP opposite to the branch guanosine when they misread the branch guanosine from the 2′-arm. When the RTs misread the branchpoint from the 3′-arm, they skipped the branched nucleotide during DNA synthesis. Notably, due to a single point mutation in RT's RNase H active site, RNase H-deficient RT misincorporated less frequently dGMP opposite to the branch guanosine than the wild-type RT when the enzymes encountered the branchpoint from the 2′-arm (Table 1).

Sequencing of cloned amplicons of arm-specific DNAs/RNAs also revealed that the polymerases can bypass the branchpoint in an error-free manner by inserting the correct partner, (d)CMP (Table 1). To our surprise, Taq and T7 RNAP do not misread the branchpoint from the 3′-arm at all. In general, an error-free branchpoint bypass was unexpected because previous data had shown that a branchpoint is highly mutagenic (Vogel et al. 1997; Tuschl et al. 1998; Vogel and Börner 2002; Gao et al. 2008; Döring and Hurek 2017).

Blocking of DNA synthesis by the branchpoint is more pronounced when polymerization proceeds from the 2′-arm than from the 3′-arm

In our present study, we primed DNA and RNA synthesis from the 2′- or 3′-arm of bDNA. In both cases only a small fraction of full-length products was generated by the polymerases from bDNA because the branchpoint was an obstacle to synthesis. We asked whether the branchpoint blocks nucleic acid synthesis from the two arms in the same manner. To address this question, we performed qPCRs on bDNA from both arms and on control DNAs as reference. Control DNA contains exclusively 3′,5′ linkages and has the same sequence (5′-segment and 2′- or 3′-arm) as the bDNA template. To explore the blocking effect of a linear 2′,5′ linkage on DNA synthesis (Lorsch et al. 1995;

TABLE 1. Transversion, deletion, and no mutation frequencies at the branchpoint found in arm-specific, full-length DNAs and RNAs after cloning

	Mutation frequency (%)[a]					
	2′-arm			3′-arm		
Nucleic acid polymerase	Transversion G→C[b]	Deletion[c]	No mutation[d]	Transversion G→C	Deletion	No mutation
Taq DNA polymerase[e]	2.2	2.2	95.7	n.d.[f]	n.d.	100
T7 RNA polymerase[e]	15.4	n.d.	84.6	n.d.	n.d.	100
Wild-type M-MLV RT[g]	39.7 ± 5.2 (A)[h]	1.6 ± 1.4 (C)	56.5 ± 4.1 (D)	n.d.	7.2 ± 3.0 (A)	93.1 ± 3.5 (B)
RNase H-deficient M-MLV RT[g]	14.9 ± 4.4 (B)	0.9 ± 1.6 (C)	83.4 ± 3.0 (E)	n.d.	6.6 ± 2.2 (A)	91.2 ± 0.3 (B)

[a]The mutation frequency was determined by sequence analysis of cloned PCR products (25–48 clones each) obtained from one or three independent experiments listed in Supplemental Tables S1–S8.
[b]Qnly unambiguous transversions at the branchpoint position in the sense-strand were included.
[c]Only unambiguous deletion mutations at the branchpoint position in the sense-strand were included.
[d]The correct nucleotide (guanosine monophosphate) was found at the position of the branchpoint in the sense-strand.
[e]The mutation frequency was obtained from one experiment.
[f]n.d., not detected.
[g]The mutation frequency was obtained from three independent experiments. Mean ± SD; SD, standard deviation.
[h]Values followed by different letters in parentheses are significantly different from each other at $P < 0.05$, according to unpaired *t*-tests with Welch's correction. Values followed by identical letters are not significantly different from each other at $P > 0.05$.The mutation frequencies by wild-type and RNase H-deficient M-MLV RT were compared for the two arms separately.

Döring and Hurek 2017), we also carried out qPCRs on precursor 1 containing a 2′,5′-linked ribo-G-nucleoside (Fig. 1). We generated standard curves of bDNAs, precursor 1, and control DNAs using equal copy numbers of templates (from 6.0×10^7 to 6.0×10^4 copies). Quantitative PCR from the 2′-arm (2_5 qPCR) was carried out using the forward and 2–5 reverse primers, and from the 3′-arm (3_5 qPCR) with the forward and 3–5 reverse primers.

In the first few cycles of qPCR, direct amplification efficiency of bDNA and precursor 1 will be lower than that of the control DNA because the branchpoint and 2′,5′ linkage inhibit full-length DNA synthesis (Lorsch et al. 1995; Nogva and Rudi 2004; Döring and Hurek 2017). In contrast, amplification efficiencies of complementary full-length DNAs and PCR products will be equal among the DNA samples since amplification occurs from the same template with only 3′,5′ linkages (Nogva and Rudi 2004; Hou et al. 2010; Lin et al. 2011). The initial lower amplification efficiency of bDNA and precursor 1 resulted in higher quantification cycle (Cq) values as compared to the control DNA at each starting copy number of template DNA (Supplemental Tables S9, S10; Sikorsky et al. 2004, 2007; Hou et al. 2010; Lin et al. 2011), and caused a horizontal shift of the standard curves without modification of the slope (Supplemental Figs. S6, S7; Hou et al. 2010; Lin et al. 2011).

To assess the blocking effect of the branched nucleotide and 2′,5′ linkage on polymerase progression, we used the difference in Cq between bDNA/precursor 1 and control standard curves for quantifying the amplification of precursor 1 and bDNA relative to the control DNA (Chen et al. 2007; Lin et al. 2011). Our quantifications (Supplemental Tables S11–S13) revealed that, due to the blocking effect of the 2′,5′ phosphodiester bond, the relative amplification of precursor 1 was 4.8 ± 0.4-fold lower than that of the control DNA (Fig. 5). Interestingly, the decrease in relative amplification of bDNA was three orders of magnitude higher when amplification of bDNA was primed from the 2′-arm (29,307 ± 2518-fold) than from the 3′-arm (15.7 ± 1.2-fold) (Fig. 5). This indicates that branchpoint blocking of DNA synthesis is much stronger when the DNA polymerase encounters the branch guanosine from the 2′-arm than from the 3′-arm.

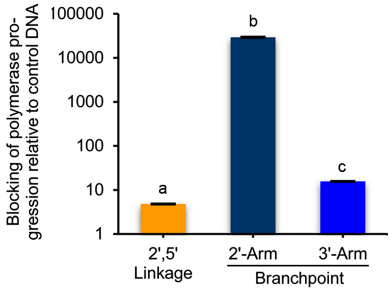

FIGURE 5. Blocking effect of 2′,5′ linkage and branchpoint on polymerase progression. Blocking of polymerase progression relative to control DNA was calculated from the $2^{\Delta Cq}{}_E$ value (Pfaffl 2001), where ΔCq_E is the difference in Cq_E (efficiency corrected Cq) between precursor 1/bDNA, and control DNA is presented using a log scale. Data points are the average of two independent experiments listed in Supplemental Tables S11–S13. Error bars *above* columns indicate standard deviations. Columns headed by different letters are significantly different from each other at $P < 0.05$ according to unpaired *t*-tests with Welch's correction.

DISCUSSION

How DNA and RNA polymerases recognize individual nucleotides is a fundamental question for understanding the molecular basis of polymerization efficiency and fidelity. Conventional approaches such as structural and computational studies have provided new insights into the molecular basis of the polymerization process (Swan et al. 2009; Berezhna et al. 2012; Freudenthal et al. 2013b). In contrast to these approaches, we utilized synthetic bDNA molecules to study the individual role of a branched nucleotide and the intrinsic structural features of nucleic acids in controlling polymerization fidelity. Using bDNA molecules, we found that Taq, M-MLV RTs, and T7 RNAP can read the branchpoint from the 2′-arm in an error-free manner by incorporating the correct partner, (d)CMP, and in an error-prone manner by incorporating (d)GMP. We also observed that the nucleic acid polymerases insert these two nucleotides with different frequencies. Taq, T7 RNAP, and RNase H-deficient RT prefer (d)CMP over (d)GMP while wild-type RT inserts dCMP and dGMP with almost equal frequencies (Fig. 6). These data indicate that the branch guanosine has a dual coding potential which is modulated by polymerases.

The coding potential of a branched nucleotide is dictated by the *anti* or *syn* conformation of the base

Similar to the oxidized guanine base [8-oxoguanine (8-oxoG)] (Uesugi and Ikehara 1977), the base of a branched nucleotide in ssRNA tri- and tetramers predominates in a mutagenic *syn* orientation (Damha and Ogilvie 1988). The same seems to apply to a branched nucleotide in long-chained RNA (Damha and Ogilvie 1988) and DNA molecules because the mutation profiles of bRNA (Döring and Hurek 2017) and bDNA are similar. The coding potential of a templating 8-oxo-dG is determined by the *syn* or *anti* conformation of the oxidized base: *anti* 8-oxoG pairs with cytosine whereas the *syn* base-pairs with adenine (Kouchakdjian et al. 1991; Oda et al. 1991; McAuley-Hecht et al. 1994; Lipscomb et al. 1995). We propose that the coding potential of a branched nucleotide depends on the same mechanism. It is conceivable that, as for 8-oxoG (Kouchakdjian et al. 1991; Oda et al. 1991; McAuley-Hecht et al. 1994; Lipscomb et al. 1995), in the case of an incoming (d)CTP, the *syn–anti* equilibrium is

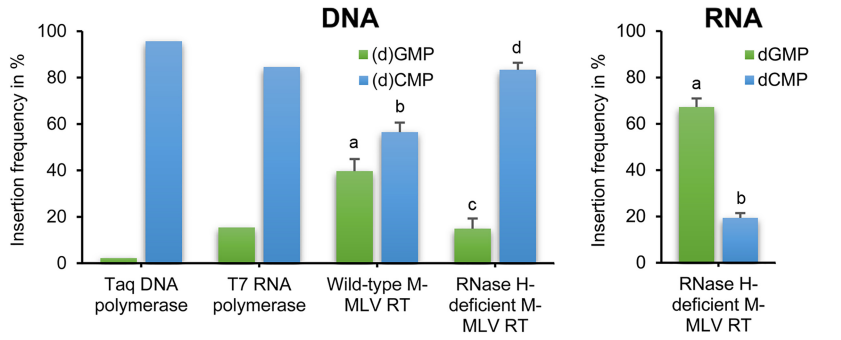

FIGURE 6. Insertion frequency of (d)GMP and (d)CMP opposite to the branch guanosine during polymerase-catalyzed nucleic acid synthesis from the 2′-arm of branched DNA (*left* panel) and RNA (*right* panel). (*Left* panel) The insertion frequency was determined by sequence analysis of cloned PCR products (37–46 clones each) listed in Supplemental Tables S1–S4. Data shown for Taq DNA and T7 RNA polymerases were obtained from one experiment and for RTs from three independent experiments. (*Right* panel) The insertion frequency was determined by sequence analysis of cloned PCR products (43–46 clones each) listed in Supplemental Table S3 (Döring and Hurek 2017). Data shown were obtained from three independent experiments. Values followed by different letters are significantly different from each other at $P < 0.05$ according to unpaired *t*-tests with Welch's correction. The insertion frequencies by RTs were compared for the two templates separately.

shifted to the *anti* branched base and the nucleobase pairs with cytosine in a normal Watson–Crick base pair. In the case of an incoming (d)GTP, the equilibrium is shifted toward the *syn* branched base and the base uses its Hoogsteen edge for mispairing with guanine (Fig. 7).

Insertion of the correct nucleotide opposite to a templating base depends on the Watson–Crick geometry of the nascent base pair in the polymerase binding pocket (Kunkel and Bebenek 2000). Similar to an 8-oxo-dG·dAMP mispair (Kouchakdjian et al. 1991; McAuley-Hecht et al. 1994), Taq, T7 RNAP, and M-MLV RTs do not recognize the misincorporated (d)GMP as aberrant because the branch guanosine·(deoxy)guanosine base pair may have a geometry similar to that of canonical Watson–Crick base pairs. The well-known preferential insertion of dAMP opposite to the branch adenosine of intron RNA lariats by RTs (Vogel et al. 1997; Vogel and Börner 2002; Gao et al. 2008) arguably also follows this geometric model.

Polymerase active sites can modulate the coding potential of a branched nucleotide

We suggest that polymerases modulate the coding potential of a branched nucleotide in a similar manner as for 8-oxo-dG (Krahn et al. 2003; Batra et al. 2012). Accordingly, polymerases have to capture the orientation of a templating branched base in order to incorporate the base-pairing partner into the nascent strand. Structural studies showed that polymerase active sites are adapted to capture either the *anti* or *syn* conformation, or both orientations of the templating base (Krahn et al. 2003; Brieba et al. 2004; Brieba et al. 2005; Rechkoblit et al. 2006; Zang et al. 2006; Eoff et al. 2007; Batra et al. 2012; Freudenthal et al. 2013a). This leads to a preference for inserting either the Watson–Crick or the mutagenic Hoogsteen partner, or to an equality of inserting these two nucleotides (Krahn et al. 2003; Brieba et al. 2004, 2005; Rechkoblit et al. 2006; Zang et al. 2006; Eoff et al. 2007; Batra et al. 2012; Freudenthal et al. 2013a).

We found that Taq predominantly inserts dCMP opposite to the branch guanosine during DNA synthesis from both arms. This indicates that, similar to Dpo4 DNA polymerase (Rechkoblit et al. 2006; Zang et al. 2006), the polymerase active site of Taq is adapted to capture only the *anti* branched base. Conversely, we found that T7 RNAP and RNase H-deficient RT insert up to one-fifth (d)GMP opposite to the branch guanosine during synthesis from the 2′-arm (Fig. 6). They can apparently capture

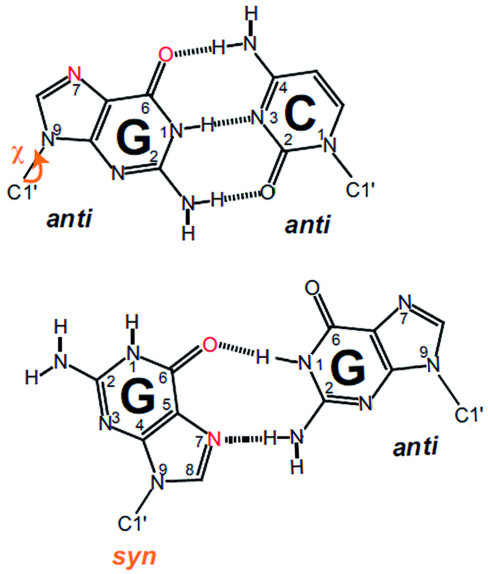

FIGURE 7. Base-pairing modes of the branch guanosine. (*Upper* panel) *Anti* branched base guanine (G) would pair with *anti* cytosine (C) through Watson–Crick base-pairing. (*Lower* panel) *Syn* branched G would pair with *anti* guanine through mutagenic Hoogsteen base-pairing. Hoogsteen hydrogen-bonding groups (Hoogsteen edge) of the branched guanine are indicated in red and the *syn* glycosidic torsion angle χ in orange. C1′ represents the 1′ carbon of the sugar. (Figure modified from Zhou et al. 2015 [by permission of Oxford University Press]; scheme of the mutagenic Hoogsteen base pair adapted from Skelly et al. 1993 [© 1993 National Academy of Sciences, USA].) Alternatively, the G-G base pair can have an additional hydrogen bond between atoms N7 of the *syn* base and N1 of the *anti* base (Skelly et al. 1993).

both orientations, but favor the *anti* branched base, which is compatible with the data obtained from T7 DNA polymerase (Brieba et al. 2004, 2005). In contrast, similar to DNA polymerase β (Krahn et al. 2003; Batra et al. 2012; Freudenthal et al. 2013a), wild-type RT apparently stabilizes both the *syn* and *anti* branched base because the enzyme incorporates dCMP and dGMP with an almost equal frequency opposite to the branch guanosine during DNA synthesis from the 2′-arm (Fig. 6).

Arm-specific bypass and blocking effect of the branchpoint

It was shown for ssRNA tri- and tetramers that the 2′-linked base stacks strongly with the branched base, whereas the 3′-linked base is totally unstacked (Damha and Ogilvie 1988; Koole et al. 1988). Because of extensive base stacking, the branchpoint and the 2′-linked nucleotide have a rigid conformation, whereas because of base unstacking, the conformation of the branchpoint and the 3′-linked nucleotide is more flexible (Damha and Ogilvie 1988). These conformational properties of the two nucleotides linking the 2′- and 3′-arms to the branched nucleotide are probably preserved in long-chained DNA and RNA since we observed an arm-specific bypass and blocking effect of the branchpoint in bRNA (Döring and Hurek 2017) and bDNA molecules.

We found that, in contrast to the 2′-arm, T7 RNAP and M-MLV RTs do not insert (d)GMP opposite to the branch guanosine during synthesis from the 3′-arm. Moreover, we found that RTs skip occasionally the branchpoint during polymerization. Apparently the conformational difference at the branchpoint leads to an inability of T7 RNAP and RTs to stabilize the templating *syn* branched base in their active sites, such that the incoming (d)GTP cannot be inserted into the nascent strand during synthesis from the 3′-arm. Furthermore, the unstacking of the 3′-linked base in the template strand can also explain why the branched nucleotide is deleted during DNA synthesis by RTs. Strand slippage can occur in response to an unstacked template base (Manjari et al. 2014) resulting in deletion mutations during DNA synthesis by DNA polymerases (Kunkel 2004, 2009). Similar deletion mutations were also obtained when RTs encounter the branchpoint from the 3′-arm of bRNA (Tuschl et al. 1998; Döring and Hurek 2017).

Our qPCR analysis showed that blocking is 1871-fold stronger when the DNA polymerase bypasses the branch guanosine from the 2′-arm than from the 3′-arm. The finding that the efficiency of reading through the 2′,5′-branch is lower than through the 3′,5′-branch, is also seen in our analysis of full-length nucleic acid generated by RTs, Taq and T7 RNAP. Consistent with our previous study on bRNA (Döring and Hurek 2017), full-length products through the 2′,5-branch were hardly visible in gels in contrast to full-length products through the 3′,5-branch (Figs. 3B, 4, Supplemental Fig. S2). We, therefore, propose that regardless of the polymerizing enzyme and regardless of whether the branchpoint is within RNA or DNA, the branchpoint blocking effect on synthesis is always stronger when polymerases encounter the branched nucleotide from the 2′-arm than from the 3′-arm. This branchpoint blocking effect is probably related to the conformational difference between the 2′,5′- and 3′,5′-linked nucleotides: The rigid conformation is difficult to bypass, whereas the flexible conformation is easier to bypass.

RT's RNase H active site modulates the coding potential of the branched guanine base

Crystal structures of RT bound to double-stranded nucleic acids revealed that the distance in nucleotides between the DNA polymerase and RNase H active sites is 17–18 base pairs (Jacobo-Molina et al. 1993; Sarafianos et al. 2001). We found that due to a single point mutation in M-MLV RT's RNase H active site, the enzyme inserts to a lower extent dGMP opposite to the branch guanosine during DNA synthesis from the 2′-arm than the wild-type enzyme (Fig. 6). Presumably, RT's polymerase active site fails to stabilize the templating *syn* branched base, such that the incoming dGTP is only rarely inserted into the nascent strand. The finding that the RNase H active site residue has a destabilizing effect on the *syn* conformation of the branched base is unexpected as RNase H is located away from the nascent base pair binding pocket. However, it was proposed that amino acid mutations that do not contact DNA or dNTP indirectly alter the geometry of the binding pocket (Kunkel and Bebenek 2000). Similarly (Kunkel and Bebenek 2000), the mutation in RT RNase H may indirectly relocate the polymerase active site residues that make stabilizing contacts with the *syn* branched base, and thus the stability of this base is decreased in the active site. Our observation that RT's RNase H active site residues have an impact on DNA synthesis is compatible with the results reported by Álvarez et al. (2013). They demonstrated that a point mutation in human immunodeficiency virus 1 RT RNase H active site increases the accuracy of RT's polymerase (Álvarez et al. 2013).

Nucleic acid-specific coding potential of the branchpoint

We noticed that when the branch guanosine is present in an RNA template, M-MLV RT (H−) undergoes error-prone branchpoint bypass (Fig. 6; Döring and Hurek 2017), whereas when it is embedded in a DNA template, the enzyme undergoes mainly error-free branchpoint bypass (Fig. 6). We conclude from these results that the type of the surrounding nucleic acid (RNA or DNA) determines which conformation of the templating branched base

(*syn* or *anti*) is stabilized in the RT polymerase active site. It was found that the polymerase RNA interaction differs from that between the polymerase and DNA. RT polymerase active sites make more extensive contacts with an RNA template than with a DNA template (Ding et al. 1997; Sarafianos et al. 2001; Nowak et al. 2013; Das et al. 2014). The palm and fingers subdomains additionally interact with the RNA template 2′ hydroxyls down and upstream of the templating nucleotide (Nowak et al. 2013). These additional interactions of the RNA with the subdomains probably result in a rigid RNA sugar-phosphate backbone. Because these interactions are absent with a DNA template (Ding et al. 1997; Das et al. 2014), it is conceivable that the DNA sugar-phosphate backbone is more flexible.

Damha and Ogilvie (1988) found that the *syn* branched base is engaged in an intramolecular base–sugar interaction. Similar to what was observed for 8-oxo-dG (Krahn et al. 2003; Rechkoblit et al. 2006; Zang et al. 2006), in the case of an incoming dCTP, the sugar-phosphate backbone upstream of the templating branched base probably has to flip ∼180° to disrupt the intramolecular *syn* base-backbone interaction. Since DNA template nucleotides have no additional contacts with the RT polymerase active site, the DNA backbone can rotate and the branched base can adopt the *anti* conformation to pair with cytosine. In contrast, the additional contacts with the 2′ hydroxyls hinder the rotation of the RNA backbone and the branched base would fail to adopt the *anti* orientation. As a consequence, the branched base would retain the mutagenic *syn* conformation and template only for the insertion of dGMP.

Because our results showed that a branchpoint in DNA is not as highly mutagenic as in RNA, it is conceivable that the intrinsic flexibility of DNA and the intrinsic rigidity of RNA (Saenger 1984) impacts the coding potential of branched nucleotides. Accordingly, DNA confers flexibility to the branched base, the flexible base is free to adopt an *anti* or *syn* orientation and pairs with the correct or incorrect partner, respectively. In contrast, RNA confers rigidity to the branched base which is forced to remain in the mutagenic *syn* conformation and pairs with an incorrect nucleotide.

Potential biological consequences of 2′,5′-linked ribonucleotides in DNA on the cellular life cycle

Ribonucleoside monophosphates (rNMPs) are occasionally incorporated into DNA genomes during replication (Williams and Kunkel 2014; Williams et al. 2016). A backbone heterogeneity with 2′,5′-linked RNA is thought to exist in DNA during molecular evolution (Xu et al. 2015). Whether contemporary template-dependent nucleic acid polymerases still tolerate 2′,5′-linked rNMPs in DNA (Xu et al. 2014, 2015) has become of interest. Our qPCR data showed that a single 2′,5′-linked ribonucleotide in a DNA template decreases DNA synthesis by a factor of 5. Consistent with the findings of Xu et al. (2014, 2015), these data indicate that 2′,5′-linked ribonucleotides in genomic DNA templates would slow down DNA replication and transcription in prokaryotic and eukaryotic cells. Moreover, because RNA 2′,5′ linkages are not a substrate for RNase H (Kandimalla et al. 1997), it is likely that such rNMPs would not be removed by the cellular type 2 RNase H-initiated repair mechanism (Williams and Kunkel 2014; Williams et al. 2016) and would persist in DNA.

In conclusion, we succeeded in constructing long chained bDNA oligonucleotides by splinted ligation. Using qPCR analysis, we found that the branchpoint blocking effect on DNA synthesis is more pronounced when the DNA polymerase encounters the branch guanosine from the 2′-arm than from the 3′-arm. Arm-specific blocking by the branchpoint may attribute to a conformational disparity of 2′,5′- and 3′,5′-linked nucleotides. We evaluated the arm-specific full-length complementary nucleic acids generated by Taq, M-MLV RTs, and T7 RNAP from our bDNA. We found that the branch guanosine templates for the insertion of (d)CMP and (d)GMP during synthesis from the 2′-arm. The dual coding potential of the branchpoint is explained by the *anti* or *syn* orientation of the branched base. We propose that polymerases and RNase H modulate the coding potential by determining which conformation of the branched base is stabilized in the polymerase active site. Furthermore, we observed that the coding potential of the branchpoint is dependent on the type of the surrounding nucleic acid. This result is explained by the different intrinsic flexibility of RNA and DNA, and also to a different interaction with RT's polymerase. In contrast to the 2′-arm, our sequence analysis of 3′-arm-specific full-length complementary nucleic acids showed a predominantly error-free branchpoint bypass by the polymerases. Nielsen and Johansen (2007) wondered whether there might be branching activity on genomic DNA. Our data would implicate that branched nucleotides resulting from this activity would be not as mutagenic as their counterparts in RNA and would hamper DNA replication and transcription.

MATERIALS AND METHODS

General

Oligonucleotides and probes used in this study can be found in Table 2. Negative controls were performed simultaneously without adding the enzyme. Ethanol precipitation of nucleic acids was done with Pellet Paint Co-Precipitant following the manufacturer's instructions (Merck Millipore) and resuspended in TE buffer (10 mM Tris-HCl, 1 mM EDTA, pH 8.0). To purify nucleic acids from polyacrylamide gels, the gel slice nutated in three volumes of TE buffer at 37°C overnight and gel-purified nucleic acids were ethanol precipitated. To purify transcripts from a denaturing polyacrylamide gel, the gel slice nutated in two volumes of elution buffer

TABLE 2. List of oligonucleotides used in this study

Oligonucleotide[a]	Sequence[b] (5′ to 3′)
Oligonucleotide with a 2′,5′ linkage (60), precursor 1	CTGTAAGAACACTAAGACGCTCGAACGGCGCGCCG GG**2′,5′**GATCCTCTAGAGTCGACCTGCAC[c]
5′-phosphorylated oligonucleotide (59), precursor 2[d]	CGAGATGCCAGCGCTACCGTCGTCTGAGGTCTTAGT GTTCTTGAACACGGTCGCGAGAG
5′-phosphorylated oligonucleotide containing the reverse complement of the T7 promoter (83), precursor 2-T7[e]	CGAGATGCCAGCGCTACCGTCGTCTGAGGTCTTAGT GTTCTTGAACACGGTCGCGAGAGTCTCCCTATAGTG AGTCGTATTAC
Bridge oligonucleotide (50)	CAGACGACGGTAGCGCTGGCATCTCGCCCGGCGCG CCGTTCGAGCGTCTT
Forward primer (20)	CTGTAAGAACACTAAGACGC
2-5 reverse primer (16)	GTGCAGGTCGACTCTA
3-5 reverse primer (21)	ACCGTGTTCAAGAACACTAAG
Oligonucleotide representing DNA until the 2′,5′ linkage and 2′,5′-branch (23)	GTGCAGGTCGACTCTAGAGGATC
Oligonucleotide representing DNA until the 3′,5′-branch (51)	ACCGTGTTCAAGAACACTAAGACCTCAGACGACGGT AGCGCTGGCATCTCG
Oligonucleotide representing full-length DNA through the 2′,5′ linkage and 2′,5′-branch (60)	GTGCAGGTCGACTCTAGAGGATCCCCGGCGCGCCG TTCGAGCGTCTTAGTGTTCTTACAG
Oligonucleotide representing full-length DNA through the 3′,5′-branch (88)	ACCGTGTTCAAGAACACTAAGACCTCAGACGACGGT AGCGCTGGCATCTCGCCCGGCGCGCCGTTCGAGC GTCTTAGTGTTCTTACAG
5′-phosphorylated T7 linker containing a 2′,3′-dideoxycytosine at the 3′-end (24)	TCTCCCTATAGTGAGTCGTATTAC
T7 primer (23)	TAATACGACTCACTATAGGGAGA
Oligonucleotide with the sequence of the bDNA construct without 3′-arm (60)	CTGTAAGAACACTAAGACGCTCGAACGGCGCGCCG GGGATCCTCTAGAGTCGACCTGCAC
Oligonucleotide with the sequence of the bDNA construct without 2′-arm (96)	CTGTAAGAACACTAAGACGCTCGAACGGCGCGCCG GGCGAGATGCCAGCGCTACCGTCGTCTGAGGTCTTA GTGTTCTTGAACACGGTCGCGAGAG
Probe O[f] (50)	CAGACGACGGTAGCGCTGGCATCTCGCCCGGCGCG CCGTTCGAGCGTCTT
Probe fl[g] (36)	CTGTAAGAACACTAAGACGCTCGAACGGCGCGCCG G

[a]Oligonucleotides were purchased from Eurofins MWG Operon unless stated otherwise. The nucleotide length of each oligonucleotide is indicated in parentheses.
[b]The underline shows the reverse complementary sequence of the T7 promoter.
[c]The magenta nucleotide represents the ribonucleotide which is connected via a 2′,5′ phosphodiester bond to the succeeding deoxynucleotide.
[d]Oligonucleotide was synthesized by Eurogentec.
[e]Oligonucleotide was purchased from Integrated DNA Technologies (IDT).
[f]Probe was labeled with digoxigenin at the 5′-end.
[g]Probe was labeled with digoxigenin at the 5′- and 3′-end.

(500 mM urea, 5 mM Tris-HCl pH 7.2, and 2 mM EDTA pH 8.0) at 37°C for 1 h. To prevent absorption of the small amount of RNA to the tube wall, the elution buffer was mixed with 2 pmol of forward primer. Gel-purified transcripts were ethanol precipitated. PCR was performed in 50 µL containing 1× Go Taq reaction buffer (Promega), 0.05 mM dNTPs (Life Technologies), 25 pmol each of the forward and 2–5 or 3–5 reverse primers, and 1.25 units of GoTaq Polymerase (Promega). The PCR consisted of an initial denaturation step at 94°C for 2 min, a PCR cycle of 94°C for 30 sec, 62.5°C for 30 sec, 72°C for 30 sec, and a final extension step at 72°C for 5 min. The PCR cycle number was dependent on the input template (see below). Five microliters of the PCR reaction was mixed with 0.5 µL 10× loading-dye (25% Ficoll-400 and 0.4% xylene cyanol) and electrophoresed on a 4% agarose gel in 1× TAE buffer (40 mM Tris-acetate and 1 mM EDTA, pH 8.3). Agarose gels were stained with ethidium bromide solution (0.5 µg/mL) and imaged by the Typhoon FLA 9500 (GE Healthcare). DNA was quantified by UV absorbance using a Nanodrop spectrophotometer (NanoDrop 2000, Thermo Scientific). To prepare double-stranded (ds) oligonucleotides, two complementary single strands (200 fmol each) were mixed in a final volume of 5 µL TE buffer containing 60 mM NaCl. The mixture was heated to 94°C for 10 sec, cooled down fast to 78°C, and then allowed to cool slowly to 27°C. Between 20 and 100 fmol of ss oligonucleotides as well as 25 and 100 fmol of ds oligonucleotides were used for gel electrophoresis analysis. Single-stranded oligonucleotides synthesized by Eurofins MWG Operon or a Low Molecular Weight DNA Ladder (New England BioLabs, NEB) were used as size markers in gel electrophoresis. Size markers in base pairs (bp) or in nucleotides (nt) are indicated on the left of the gel. All experiments were repeated at least twice if not stated otherwise.

Polyacrylamide gel electrophoresis

Denaturing polyacrylamide gels were prepared with either 10 or 15% acrylamide, 0.17% N,N′-methylenebisacrylamide, 8 M urea in 1× TBE buffer (89 mM each Tris-base and boric acid, 2 mM EDTA, pH 8.3). Two volumes of urea loading buffer (8 M urea, 50 mM Tris-HCl, pH 7.5, and 20 mM EDTA, pH 8.0) were added to the samples and the mixtures were heated at 70°C for 10 min before loading. Native polyacrylamide gels were prepared with either 12% or 15% acrylamide, 0.17% N, N′-methylenebisacrylamide in 1× TBE buffer. For denaturing electrophoresis, samples were mixed with two volumes of formamide loading-dye (90% de-ionised formamide, 50 mM Tris-HCl, pH 7.2, and 20 mM EDTA, pH 8.0), heated at 94°C for 10 sec, and snap-cooled on ice before loading. For nondenaturing electrophoresis, one-sixth volume of Gel loading dye, Blue (6×) (NEB) was added to the samples. All gel electrophoreses were carried out according to standard protocols. Gels were stained with SYBR Gold as per manufacturer's instructions (Life Technologies) and imaged by the Typhoon FLA 9500 (GE Healthcare).

Hybridization analysis

After denaturing gel electrophoresis, nucleic acids were transferred by capillary transfer with 20× SSC buffer (3 M NaCl and 0.3 M sodium citrate, pH 7.0) overnight to a positively charged nylon membrane (GE Healthcare Life Sciences). After nondenaturing gel electrophoresis, nucleic acids were blotted by capillary transfer in denaturation solution (1.5 M NaCl and 0.5 M sodium hydroxide) overnight onto a positively charged nylon membrane (GE Healthcare Life Sciences). The membrane was treated with neutralization solution (0.5 M Tris-HCl, pH 7.5, 1.5 M NaCl) before

hybridization. Membranes were incubated with the digoxigenin-labeled probe in hybridization buffer (5× SSC buffer, 5× Denhardt's solution, and 0.5% SDS) at the hybridization temperature (probe O at 70°C and probe fl at 65°C) overnight. After sequential wash in 5× SSC buffer containing 0.1% SDS, 2× SSC buffer containing 0.1% SDS, and 0.1× SSC buffer containing 0.1% SDS at the hybridization temperature for 15 min, blots were developed using alkaline phosphatase-conjugated anti-digoxigenin antibody and the chemiluminescent substrate CDP-Star according to the manufacturer's instructions (Roche Life Science). Chemiluminescent signals were imaged using the Luminescent Image Analyzer LAS-3000 mini (Fujifilm Life Science).

Fusion of the complementary sequence of the T7 promoter to precursor 1

To ligate the complementary sequence of the T7 promoter to the 3′-end of precursor 1, 1 pmol of precursor 1 and 100 pmol of a 5′-phosphorylated ss oligonucleotide corresponding to the reverse complement of the T7 promoter (T7 linker) were mixed in a 20 µL volume containing 1× T4 RNA Ligase reaction buffer (NEB), 1 mM ATP (NEB), 25% (w/v) PEG 8000 (NEB), and 10 units of T4 RNA Ligase 1 (NEB). To prevent formation of concatemers, the T7 linker contained a 3′ chain terminator (2′,3′-dideoxycytosine). The reaction and negative control were incubated at 22°C overnight. Ligation of the two oligonucleotides was confirmed by gel electrophoresis (Supplemental Fig. S8). Ligation reaction was ethanol precipitated and the product (precursor 1-T7) was gel-purified using TE buffer.

Ligase-mediated construction of branched DNA

To construct bDNA oligonucleotides, we used the splinted ligation method (Fig. 1), as previously reported by Mendel-Hartvig et al. (2004). Hybridization of precursors 1 and 2 to the DNA bridge was done as previously described (Döring and Hurek 2017). To construct native bDNA, we used precursors 1 and 2. To prepare bDNA with a T7 promoter at the 2′-arm, precursor 1-T7 and precursor 2 were used. Conversely, to construct bDNA with a T7 promoter at the 3′-arm, precursor 1 and precursor 2-T7 were used. Joining of the two precursors was performed in a 20 µL volume containing 1 pmol of ds oligonucleotide from the hybridization reaction, 1× T4 DNA Ligase buffer (Thermo Scientific), 50 mM NaCl, and 5 units of T4 DNA Ligase (Thermo Scientific). The reaction and negative control were incubated at 37°C overnight and ligation of the two precursors was validated by hybridization analysis (Supplemental Fig. S9). Ligation reaction was column-purified using the NucleoSpin Gel and PCR Clean-up Kit following the manufacturer's protocol for clean-up of ssDNA (Macherey-Nagel). The eluted nucleic acids were ethanol precipitated and electrophoresed under denaturing conditions on a 15% native polyacrylamide gel to gel-purify bDNA. Gel purification of bDNA oligonucleotides was carried out twice.

In vitro transcription using T7 RNA polymerase

Single-stranded DNA templates equipped with the complementary sequence of the T7 promoter at their 3′-ends were used for in vitro transcription. To generate the double-stranded T7 promoter region, an oligonucleotide representing the T7 promoter sequence (T7 primer) was annealed to its complementary sequence on the template. To prepare the partially ds oligonucleotide, 200 fmol of template and 25 pmol of T7 primer were mixed in a final volume of 5.5 µL containing 100 mM NaCl. The mixture was heated to 94°C for 30 sec, cooled down fast to 75°C, and then allowed to cool slowly to 27°C. To this mixture was added 8 µL H_2O, 4 µL 5× Transcription buffer (Thermo Scientific), 1 µL 40 mM NTPs (Life Technologies), 0.5 µL RiboLock RNase Inhibitor (20 units) (Thermo Scientific), and 1 µL T7 RNA polymerase (20 units) (Thermo Scientific). The reaction and the negative control were incubated at 37°C for 2 h. Nucleic acids were phenol/chloroform extracted, ethanol precipitated, loaded on a 15% denaturing polyacrylamide gel, and in vitro transcribed RNA through the 2′,5′- and 3′,5′-branch was gel-purified.

RT-PCR

To generate cDNA from in vitro transcribed RNA through the 2′,5′- and 3′,5′-branch, one-fourth of the gel-purified RNA was mixed in a 25 µL volume containing 1× M-MLV RT reaction buffer (Promega), 25 pmol forward primer, 0.5 mM dNTPs (Life Technologies), and 200 units of M-MLV RT (H−) (Promega). The reaction and negative control were incubated at 42°C for 1 h, and the enzyme was heat inactivated at 70°C for 15 min. One-tenth volume of the RT reaction and negative control were subjected to 45 cycles of PCR for amplification of cDNA from in vitro transcribed RNA through the 2′,5′-branch or to 35 cycles of PCR for amplification of cDNA from in vitro transcribed RNA through the 3′,5′-branch.

Primer extension reaction and PCR

The 2–5 and 3–5 reverse primers were used for primer extension reactions from the 2′- and 3′-arms of bDNA, respectively. Two hundred fmol of template and 25 pmol of the respective reverse primer were mixed in a final volume of 6.2 µL TE buffer containing 15 mM NaCl. The mixture was heated to 94°C for 30 sec, cooled down fast to 78°C, and then cooled down slowly to 27°C.

Taq DNA polymerase

Primer extension reaction from the 2′-arm was performed in a 10 µL volume containing 1× Go Taq reaction buffer (Promega), 0.05 mM dNTPs (Life Technologies), and 1.25 units of GoTaq DNA polymerase (Promega). The reaction and negative control were incubated at 72°C for 20 min, subsequently phenol/chloroform extracted, and ethanol precipitated.

Reverse transcriptase

Primer extension reactions using either M-MLV RT (H+) or M-MLV RT (H−) (Promega) were carried out as previously described (Döring and Hurek 2017).

Samples were electrophoresed either under nondenaturing conditions on a 12% native or on a 15% denaturing polyacrylamide gel. To amplify DNAs through the 2′,5′-branch, extension products were excised from a native gel. One-fourth of the gel

slice was added to the PCR reaction mix and amplification was performed with 40 cycles. To amplify DNAs through the 3′,5′-branch generated by M-MLV RT (H+) and (H−), extension products were gel-purified from a denaturing gel. One-tenth volume of the gel-purified DNA was subjected to 30 cycles of PCR.

For PCR from the 3′-arm, 5 fmol of bDNA was used as template. To allow GoTaq DNA polymerase (Promega) to extend the primer through the branchpoint, the PCR reaction mix was initially incubated at 94°C for 30 sec, 62.5°C for 2 min, 72°C for 10 min, and then subjected to 45 cycles.

Sequencing of PCR amplicons and bioinformatic analysis

PCR products obtained from full-length DNA through the 2′,5′-branch were ethanol precipitated and gel-purified from a 15% native polyacrylamide gel. One-tenth volume of the gel-purified amplicons was used for cloning. RT-PCR amplicons obtained from in vitro transcribed RNA through the 2′,5′-branch were column-purified using the QIAquick Nucleotide Removal Kit as per manufacturer's instructions (Qiagen) and quantified. PCR and RT-PCR products obtained from full-length DNA and in vitro transcribed RNA through the 3′,5′-branch, respectively, were column-purified using the QIAquick PCR Purification Kit following the manufacturer's protocol (Qiagen) and quantified. A total of 75 fmol of column-purified PCR products was used in the cloning reaction. Cloning, sequencing, and sequence analysis of amplicons was carried out as described previously (Döring and Hurek 2017).

Statistical analysis

Statistical analysis was performed with GraphPad Prism v7.03 (Graphpad software). Data were analyzed using unpaired *t*-tests with Welch's correction not assuming equal standard deviations.

qPCR

Quantitative real-time PCR is the method of choice to investigate the effect of DNA damage (Sikorsky et al. 2004, 2007) and plasmid DNA conformation (Chen et al. 2007; Hou et al. 2010; Lin et al. 2011) on PCR amplification. We used this method to explore the effect of a 2′,5′ linkage and a branchpoint on polymerase progression. Quantitative PCR through the 2′,5′ linkage of linear and bDNA is designated as 2_5 qPCR and through the 3′,5′ linkage of the branchpoint as 3_5 qPCR. Quantitative PCR was performed on a CFX96 Touch (BioRad) using SsoAdvanced SYBR Green Supermix according to the manufacturer's instructions (BioRad). The reaction mixture contained 0.3 µM each of the forward and 2–5 or 3–5 reverse primers. The qPCR was as follows: 94°C for 30 sec, 62.5°C for 2 min, 72°C for 10 min (94°C for 30 sec, 62.5°C for 30 sec, 72°C for 30 sec) × 45 cycles. To verify that a single PCR product was obtained, a melt curve analysis was carried out for each sample at the end of amplification (Ririe et al. 1997). Melt curve analysis was performed from 55°C to 95°C at increments of 0.5°C for 30 sec. To prepare standard curves, oligonucleotides were serially diluted (from 6.0×10^7 to 6.0×10^4 copies/µL) in TE buffer containing 10 ng/µL poly(A) RNA (Carrier RNA, Qiagen). A standard curve was conducted using 1 µL of each dilution for qPCR. Standard curves were generated from precursor 1, bDNA and oligonucleotides containing only 3′,5′ linkages and the same sequence (5′-segment and 2′- or 3′-arm) as the bDNA template. No template controls (NTCs) were supplied with 10 ng poly(A) RNA. Quantitative PCR of standards and NTCs were performed in triplicate and the data were analyzed by CFX Manager software (BioRad). Amplification and standard curves of DNA samples, as well as melt peaks of amplicons are shown in Supplemental Figs. S6 and S7. The software calculated amplification efficiency of PCR reactions (defined as percentage from 0% to 100%), the coefficient of determination, the slope and the Y-intercept are indicated for each standard curve. Quantification cycle values were determined by using regression. To calculate arm-specific and 2′,5′-linkage blocking, we used efficiency corrected mean Cq values from two independent experiments. The efficiency corrected Cq (Cq_E) was calculated by the following formula: $Cq_E = Cq\ mean \times \log_2 10^{(-1/slope)}$ (Karlen et al. 2007; Yuan et al. 2008). The amplification of precursor 1 and bDNA relative to the control DNA is expressed as $2^{\Delta CqE}$ (Pfaffl 2001), where ΔCq_E is the Cq_E difference between precursor 1 or bDNA standard and control standard across serial dilutions.

SUPPLEMENTAL MATERIAL

Supplemental material is available for this article.

ACKNOWLEDGMENTS

We are grateful to Sina Duschek for expert technical assistance in preparing the clone libraries and quantitative real-time PCRs. We thank Professor Reimer Stick for critical reading of the manuscript and for his helpful suggestions, and Dr. Claudia Sofía Burbano for careful reading of the manuscript. We are indebted to Professor Barbara Reinhold-Hurek for provision of laboratory facilities and support.

Received August 22, 2018; accepted October 15, 2018.

REFERENCES

Álvarez M, Barrioluengo V, Afonso-Lehmann RN, Menéndez-Arias L. 2013. Altered error specificity of RNase H-deficient HIV-1 reverse transcriptases during DNA-dependent DNA synthesis. *Nucleic Acids Res* **41:** 4601–4612. doi:10.1093/nar/gkt109

Batra VK, Shock DD, Beard WA, McKenna CE, Wilson SH. 2012. Binary complex crystal structure of DNA polymerase β reveals multiple conformations of the templating 8-oxoguanine lesion. *Proc Natl Acad Sci* **109:** 113–118. doi:10.1073/pnas.1112235108

Beckman KB, Ames BN. 1997. Oxidative decay of DNA. *J Biol Chem* **272:** 19633–19636. doi:10.1074/jbc.272.32.19633

Berezhna SY, Gill JP, Lamichhane R, Millar DP. 2012. Single-molecule Förster resonance energy transfer reveals an innate fidelity checkpoint in DNA polymerase I. *J Am Chem Soc* **134:** 11261–11268. doi:10.1021/ja3038273

Bitton DA, Rallis C, Jeffares DC, Smith GC, Chen YY, Codlin S, Marguerat S, Bähler J. 2014. LaSSO, a strategy for genome-wide mapping of intronic lariats and branch points using RNA-seq. *Genome Res* **24:** 1169–1179. doi:10.1101/gr.166819.113

Brieba LG, Eichman BF, Kokoska RJ, Doublié S, Kunkel TA, Ellenberger T. 2004. Structural basis for the dual coding potential

of 8-oxoguanosine by a high-fidelity DNA polymerase. *EMBO J* **23:** 3452–3461. doi:10.1038/sj.emboj.7600354

Brieba LG, Kokoska RJ, Bebenek K, Kunkel TA, Ellenberger T. 2005. A lysine residue in the fingers subdomain of T7 DNA polymerase modulates the miscoding potential of 8-oxo-78-dihydroguanosine. *Structure* **13:** 1653–1659. doi:10.1016/j.str.2005.07.020

Cazenave C, Uhlenbeck OC. 1994. RNA template-directed RNA synthesis by T7 RNA polymerase. *Proc Natl Acad Sci* **91:** 6972–6976. doi:10.1073/pnas.91.15.6972

Cheetham GM, Steitz TA. 2000. Insights into transcription: structure and function of single-subunit DNA-dependent RNA polymerases. *Curr Opin Struct Biol* **10:** 117–123. doi:10.1016/S0959-440X(99)00058-5

Chen J, Kadlubar FF, Chen JZ. 2007. DNA supercoiling suppresses real-time PCR: a new approach to the quantification of mitochondrial DNA damage and repair. *Nucleic Acids Res* **35:** 1377–1388. doi:10.1093/nar/gkm010

Cheng Z, Menees TM. 2004. RNA branching and debranching in the yeast retrovirus-like element Ty1. *Science* **303:** 240–243. doi:10.1126/science.1087023

Conklin JF, Goldman A, Lopez AJ. 2005. Stabilization and analysis of intron lariats in vivo. *Methods* **37:** 368–375. doi:10.1016/j.ymeth.2005.08.002

Coombes CE, Boeke JD. 2005. An evaluation of detection methods for large lariat RNAs. *RNA* **11:** 323–331. doi:10.1261/rna.7124405

Cramer P. 2002. Multisubunit RNA polymerases. *Curr Opin Struct Biol* **12:** 89–97. doi:10.1016/S0959-440X(02)00294-4

Damha MJ, Ogilvie KK. 1988. Conformational properties of branched RNA fragments in aqueous solution. *Biochemistry* **27:** 6403–6416. doi:10.1021/bi00417a032

Das K, Martinez SE, Bandwar RP, Arnold E. 2014. Structures of HIV-1 RT-RNA/DNA ternary complexes with dATP and nevirapine reveal conformational flexibility of RNA/DNA: insights into requirements for RNase H cleavage. *Nucleic Acids Res* **42:** 8125–8137. doi:10.1093/nar/gku487

Ding J, Hughes SH, Arnold E. 1997. Protein-nucleic acid interactions and DNA conformation in a complex of human immunodeficiency virus type 1 reverse transcriptase with a double-stranded DNA template-primer. *Biopolymers* **44:** 125–138. doi:10.1002/(SICI)1097-0282(1997)44:2<125::AID-BIP2>3.0.CO;2-X

Döring J, Hurek T. 2017. Arm-specific cleavage and mutation during reverse transcription of 2′5′-branched RNA by Moloney murine leukemia virus reverse transcriptase. *Nucleic Acids Res* **45:** 3967–3984. doi:10.1093/nar/gkx073

Eoff RL, Irimia A, Angel KC, Egli M, Guengerich FP. 2007. Hydrogen bonding of 78-dihydro-8 oxodeoxyguanosine with a charged residue in the little finger domain determines miscoding events in *Sulfolobus solfataricus* DNA polymerase Dpo4. *J Biol Chem* **282:** 19831–19843. doi:10.1074/jbc.M702290200

Freudenthal BD, Beard WA, Wilson SH. 2013a. DNA polymerase minor groove interactions modulate mutagenic bypass of a templating 8-oxoguanine lesion. *Nucleic Acids Res* **41:** 1848–1858. doi:10.1093/nar/gks1276

Freudenthal BD, Beard WA, Shock DD, Wilson SH. 2013b. Observing a DNA polymerase choose right from wrong. *Cell* **154:** 157–168. doi:10.1016/j.cell.2013.05.048

Galvis AE, Fisher HE, Fan H, Camerini D. 2017. Conformational changes in the 5′ end of the HIV-1 genome dependent on the debranching enzyme DBR1 during early stages of infection. *J Virol* **91:** e01377-17. doi:10.1128/JVI.01377-17

Gao K, Masuda A, Matsuura T, Ohno K. 2008. Human branch point consensus sequence is yUnAy. *Nucleic Acids Res* **36:** 2257–2267. doi:10.1093/nar/gkn073

Hou Y, Zhang H, Miranda L, Lin S. 2010. Serious overestimation in quantitative PCR by circular supercoiled plasmid standard: microalgal *pcna* as the model gene. *PLoS One* **5:** e9545. doi:10.1371/journal.pone.0009545

Hsu MY, Inouye S, Inouye M. 1989. Structural requirements of the RNA precursor for the biosynthesis of the branched RNA-linked multicopy single-stranded DNA of *Myxococcus xanthus*. *J Biol Chem* **264:** 6214–6219.

Jacobo-Molina A, Ding J, Nanni RG, Clark AD Jr, Lu X, Tantillo C, Williams RL, Kamer G, Ferris AL, Clark P, et al. 1993. Crystal structure of human immunodeficiency virus type 1 reverse transcriptase complexed with double-stranded DNA at 30 Å resolution shows bent DNA. *Proc Natl Acad Sci* **90:** 6320–6324. doi:10.1073/pnas.90.13.6320

Joyce CM, Steitz TA. 1995. Polymerase structures and function: variations on a theme? *J Bacteriol* **177:** 6321–6329. doi:10.1128/jb.177.22.6321-6329.1995

Kandimalla ER, Manning A, Zhao Q, Shaw DR, Byrn RA, Sasisekharan V, Agrawal S. 1997. Mixed backbone antisense oligonucleotides: design biochemical and biological properties of oligonucleotides containing 2′-5′-ribo- and 3′-5′-deoxyribonucleotide segments. *Nucleic Acids Res* **25:** 370–378. doi:10.1093/nar/25.2.370

Karlen Y, McNair A, Perseguers S, Mazza C, Mermod N. 2007. Statistical significance of quantitative PCR. *BMC Bioinformatics* **8:** 131. doi:10.1186/1471-2105-8-131

Koole LH, Buck HM, Kuijpers WHA, Balgobin N, Nyilas A, Remaud G, Vial J-M, Chattopadhyaya J. 1988. Lariat formation in splicing of pre-messenger RNA conformation and base stacking at the lariat branch point studied using 500-MHz ^{1}H NMR and CD spectroscopy. *Recl Trav Chim Pays-Bas* **107:** 663–667. doi:10.1002/recl.19881071203

Kornberg A, Baker TA. 1992. *DNA replication*, 2nd ed. W.H. Freeman and Co., New York, NY.

Kouchakdjian M, Bodepudi V, Shibutani S, Eisenberg M, Johnson F, Grollman AP, Patel DJ. 1991. NMR structural studies of the ionizing radiation adduct 7-hydro-8-oxodeoxyguanosine (8-oxo-7H-dG) opposite deoxyadenosine in a DNA duplex. 8-Oxo-7H-dG(syn).dA(anti) alignment at lesion site. *Biochemistry* **30:** 1403–1412. doi:10.1021/bi00219a034

Krahn JM, Beard WA, Miller H, Grollman AP, Wilson SH. 2003. Structure of DNA polymerase β with the mutagenic DNA lesion 8-oxodeoxyguanine reveals structural insights into its coding potential. *Structure* **11:** 121–127. doi:10.1016/S0969-2126(02)00930-9

Krainer AR, Maniatis T, Ruskin B, Green MR. 1984. Normal and mutant human β-globin pre-mRNAs are faithfully and efficiently spliced in vitro. *Cell* **36:** 993–1005. doi:10.1016/0092-8674(84)90049-7

Kruger K, Grabowski PJ, Zaug AJ, Sands J, Gottschling DE, Cech TR. 1982. Self-splicing RNA: autoexcision and autocyclization of the ribosomal RNA intervening sequence of *Tetrahymena*. *Cell* **1:** 147–157. doi:10.1016/0092-8674(82)90414-7

Kunkel TA. 2004. DNA replication fidelity. *J Biol Chem* **279:** 16895–16898. doi:10.1074/jbc.R400006200

Kunkel TA. 2009. Evolving views of DNA replication infidelity. *Cold Spring Harb Symp Quant Biol* **74:** 91–101. doi:10.1101/sqb.2009.74.027

Kunkel TA, Bebenek K. 2000. DNA replication fidelity. *Annu Rev Biochem* **69:** 497–529. doi:10.1146/annurev.biochem.69.1.497

Le Grice SFJ, Nowotny M. 2014. Reverse transcriptases. In *Nucleic acid polymerases* (ed. Murakami KS and Trakselis MA), pp. 189–214. Springer-Verlag, Berlin/Heidelberg, Germany.

Lehmann E, Brueckner F, Cramer P. 2007. Molecular basis of RNA-dependent RNA polymerase II activity. *Nature* **450:** 445–449. doi:10.1038/nature06290

Lin CH, Chen YC, Pan TM. 2011. Quantification bias caused by plasmid DNA conformation in quantitative real-time PCR assay. *PLoS One* **6:** e29101. doi:10.1371/journal.pone.0029101

Lipscomb LA, Peek ME, Morningstar ML, Verghis SM, Miller EM, Rich A, Essigmann JM, Williams LD. 1995. X-ray structure of a DNA decamer containing 78-dihydro-8-oxoguanine. *Proc Natl Acad Sci* **92:** 719–723. doi:10.1073/pnas.92.3.719

Lorsch JR, Bartel DP, Szostak JW. 1995. Reverse transcriptase reads through a 2′-5′ linkage and a 2′-thiophosphate in a template. *Nucleic Acids Res* **23:** 2811–2814. doi:10.1093/nar/23.15.2811

Manjari SR, Pata JD, Banavali NK. 2014. Cytosine unstacking and strand slippage at an insertion-deletion mutation sequence in an overhang-containing DNA duplex. *Biochemistry* **53:** 3807–3816. doi:10.1021/bi500189g

McAuley-Hecht KE, Leonard GA, Gibson NJ, Thomson JB, Watson WP, Hunter WN, Brown T. 1994. Crystal structure of a DNA duplex containing 8-hydroxydeoxyguanine-adenine base pairs. *Biochemistry* **33:** 10266–10270. doi:10.1021/bi00200a006

Mendel-Hartvig M, Kumar A, Landegren U. 2004. Ligase-mediated construction of branched DNA strands: a novel DNA joining activity catalyzed by T4 DNA ligase. *Nucleic Acids Res* **32:** e2. doi:10.1093/nar/gnh011

Mercer TR, Clark MB, Andersen SB, Brunck ME, Haerty W, Crawford J, Taft RJ, Nielsen LK, Dinger ME, Mattick JS. 2015. Genome-wide discovery of human splicing branchpoints. *Genome Res* **25:** 290–303. doi:10.1101/gr.182899.114

Nam K, Hudson RH, Chapman KB, Ganeshan K, Damha MJ, Boeke JD. 1994. Yeast lariat debranching enzyme. Substrate and sequence specificity. *J Biol Chem* **269:** 20613–20621.

Nielsen H, Johansen SD. 2007. A new RNA branching activity: the GIR1 ribozyme. *Blood Cells Mol Dis* **38:** 102–109. doi:10.1016/j.bcmd.2006.11.001

Nielsen H, Westhof E, Johansen S. 2005. An mRNA is capped by a 2′, 5′ lariat catalyzed by a group I-like ribozyme. *Science* **309:** 1584–1587. doi:10.1126/science.1113645

Nogva HK, Rudi K. 2004. Potential influence of the first PCR cycles in real-time comparative gene quantifications. *Biotechniques* **37:** 246–253. doi:10.2144/04372RR01

Nowak E, Potrzebowski W, Konarev PV, Rausch JW, Bona MK, Svergun DI, Bujnicki JM, Le Grice SF, Nowotny M. 2013. Structural analysis of monomeric retroviral reverse transcriptase in complex with an RNA/DNA hybrid. *Nucleic Acids Res* **41:** 3874–3887. doi:10.1093/nar/gkt053

Oda Y, Uesugi S, Ikehara M, Nishimura S, Kawase Y, Ishikawa H, Inoue H, Ohtsuka E. 1991. NMR studies of a DNA containing 8-hydroxydeoxyguanosine. *Nucleic Acids Res* **19:** 1407–1412. doi:10.1093/nar/19.7.1407

Ollis DL, Brick P, Hamlin R, Xuong NG, Steitz TA. 1985. Structure of large fragment of *Escherichia coli* DNA polymerase I complexed with dTMP. *Nature* **313:** 762–766. doi:10.1038/313762a0

Padgett RA, Konarska MM, Grabowski PJ, Hardy SF, Sharp PA. 1984. Lariat RNA's as intermediates and products in the splicing of messenger RNA precursors. *Science* **225:** 898–903. doi:10.1126/science.6206566

Pfaffl MW. 2001. A new mathematical model for relative quantification in real-time RT-PCR. *Nucleic Acids Res* **29:** e45. doi:10.1093/nar/29.9.e45

Pratico ED, Silverman SK. 2007. Ty1 reverse transcriptase does not read through the proposed 2′,5′-branched retrotransposition intermediate in vitro. *RNA* **13:** 1528–1536. doi:10.1261/rna.629607

Rechkoblit O, Malinina L, Cheng Y, Kuryavyi V, Broyde S, Geacintov NE, Patel DJ. 2006. Stepwise translocation of Dpo4 polymerase during error-free bypass of an oxoG lesion. *PLoS Biol* **4:** e11. doi:10.1371/journal.pbio.0040011

Ririe KM, Rasmussen RP, Wittwer CT. 1997. Product differentiation by analysis of DNA melting curves during the polymerase chain reaction. *Anal Biochem* **245:** 154–160. doi:10.1006/abio.1996.9916

Rodriguez JR, Pikielny CW, Rosbash M. 1984. In vivo characterization of yeast mRNA processing intermediates. *Cell* **39:** 603–610. doi:10.1016/0092-8674(84)90467-7

Ruskin B, Green MR. 1985. An RNA processing activity that debranches RNA lariats. *Science* **229:** 135–140. doi:10.1126/science.2990042

Ruskin B, Krainer AR, Maniatis T, Green MR. 1984. Excision of an intact intron as a novel lariat structure during pre-mRNA splicing in vitro. *Cell* **38:** 317–331. doi:10.1016/0092-8674(84)90553-1

Saenger W. 1984. *Principles of nucleic acids structure*. Springer-Verlag, New York.

Sarafianos SG, Das K, Tantillo C, Clark AD Jr, Ding J, Whitcomb JM, Boyer PL, Hughes SH, Arnold E. 2001. Crystal structure of HIV-1 reverse transcriptase in complex with a polypurine tract RNA:DNA. *EMBO J* **15:** 1449–1461. doi:10.1093/emboj/20.6.1449

Sikorsky JA, Primerano DA, Fenger TW, Denvir J. 2004. Effect of DNA damage on PCR amplification efficiency with the relative threshold cycle method. *Biochem Biophys Res Commun* **323:** 823–830. doi:10.1016/j.bbrc.2004.08.168

Sikorsky JA, Primerano DA, Fenger TW, Denvir J. 2007. DNA damage reduces *Taq* DNA polymerase fidelity and PCR amplification efficiency. *Biochem Biophys Res Commun* **355:** 431–437. doi:10.1016/j.bbrc.2007.01.169

Skelly JV, Edwards KJ, Jenkins TC, Neidle S. 1993. Crystal structure of an oligonucleotide duplex containing GG base pairs: influence of mispairing on DNA backbone conformation. *Proc Natl Acad Sci* **90:** 804–808. doi:10.1073/pnas.90.3.804

Sousa R. 1996. Structural and mechanistic relationships between nucleic acid polymerases. *Trends Biochem Sci* **21:** 186–190. doi:10.1016/S0968-0004(96)10023-2

Swan MK, Johnson RE, Prakash L, Prakash S, Aggarwal AK. 2009. Structural basis of high-fidelity DNA synthesis by yeast DNA polymerase δ. *Nat Struct Mol Biol* **16:** 979–986. doi:10.1038/nsmb.1663

Trakselis MA, Murakami KS. 2014. Introduction to nucleic acid polymerases: families themes and mechanisms. In *Nucleic acid polymerases* (ed. Murakami KS, Trakselis MA), pp. 1–15. Springer-Verlag, Berlin/Heidelberg, Germany.

Tuschl T, Sharp PA, Bartel DP. 1998. Selection in vitro of novel ribozymes from a partially randomized U2 and U6 snRNA library. *EMBO J* **17:** 2637–2650. doi:10.1093/emboj/17.9.2637

Uesugi S, Ikehara M. 1977. Carbon-13 magnetic resonance spectra of 8-substituted purine nucleosides. Characteristic shifts for the syn conformation. *J Am Chem Soc* **99:** 3250–3253. doi:10.1021/ja00452a008

Vogel J, Börner T. 2002. Lariat formation and a hydrolytic pathway in plant chloroplast group II intron splicing. *EMBO J* **21:** 3794–3803. doi:10.1093/emboj/cdf359

Vogel J, Hess WR, Börner T. 1997. Precise branch point mapping and quantification of splicing intermediates. *Nucleic Acids Res* **15:** 2030–2031. doi:10.1093/nar/25.10.2030

Wallace JC, Edmonds M. 1983. Polyadenylylated nuclear RNA contains branches. *Proc Natl Acad Sci* **80:** 950–954. doi:10.1073/pnas.80.4.950

Williams JS, Kunkel TA. 2014. Ribonucleotides in DNA: origins repair and consequences. *DNA Repair* **19:** 27–37. doi:10.1016/j.dnarep.2014.03.029

Williams JS, Lujan SA, Kunkel TA. 2016. Processing ribonucleotides incorporated during eukaryotic DNA replication. *Nat Rev Mol Cell Biol* **17:** 350–363. doi:10.1038/nrm.2016.37

Xu L, Zhang L, Chong J, Xu J, Huang X, Wang D. 2014. Strand-specific asymmetric contribution of phosphodiester linkages on RNA polymerase II transcriptional efficiency and fidelity. *Proc Natl Acad Sci* **111:** E3269–E3276. doi:10.1073/pnas.1406234111

Xu L, Wang W, Zhang L, Chong J, Huang X, Wang D. 2015. Impact of template backbone heterogeneity on RNA polymerase II transcription. *Nucleic Acids Res* **43:** 2232–2241. doi:10.1093/nar/gkv059

Yuan JS, Wang D, Stewart CN Jr. 2008. Statistical methods for efficiency adjusted real-time PCR quantification. *Biotechnol J* **3:** 112–123. doi:10.1002/biot.200700169

Zang H, Irimia A, Choi JY, Angel KC, Loukachevitch LV, Egli M, Guengerich FP. 2006. Efficient and high fidelity incorporation of dCTP opposite 7,8-dihydro-8-oxodeoxyguanosine by *Sulfolobus solfataricus* DNA polymerase Dpo4. *J Biol Chem* **281:** 2358–2372. doi:10.1074/jbc.M510889200

Zhou H, Hintze BJ, Kimsey IJ, Sathyamoorthy B, Yang S, Richardson JS, Al-Hashimi HM. 2015. New insights into Hoogsteen base pairs in DNA duplexes from a structure-based survey. *Nucleic Acids Res* **43:** 3420–3433. doi:10.1093/nar/gkv241